fishes

MDPI

Article

TMT-Based Quantitative Proteomics Reveal the Metabolic Changes Underlying Growth Superiority in a Novel *Gymnocypris* Hybrid, *Gymnocypris przewalskii* ♀ × *G. eckloni* ♂

Yanzhen Dong, Junming Zhou *, Dayong Xu, Yun Zhao and Dongming Qi

Key Laboratory of Plateau Wetland Ecology and Environmental Protection, Xichang University, Xichang 615013, China; xcc04000019@xcc.edu.cn (Y.D.); xcc04000017@xcc.edu.cn (D.X.); 1901130065@nbu.edu.cn (Y.Z.); xcc04000029@xcc.edu.cn (D.Q.)

* Correspondence: xcc20210195@xcc.edu.cn

Abstract: Hybrid breeding is an effective approach to generate better varieties and prevent variety degradation. The present study investigated the metabolic changes underlying growth superiority in the novel *Gymnocypris* hybrid (GH), *Gymnocypris przewalskii* ♀ (GP) × *G. eckloni* ♂ (GE). The ranking of survival rate was GH > GE > GP, whereas the ranking of growth rate was GE > GH > GP. A proteomic analysis of G. hybrid and its parents was conducted to elucidate the metabolic changes underlying growth superiority. Identified pathways were primarily associated with amino acid, carbohydrate, energy, lipid, and nucleotide metabolism. These metabolic pathways, which are closely associated with growth, are controlled through regulation of the expression of numerous proteins, including adenosylhomocysteinase, hydroxypyruvate reductase, glutamate-cysteine ligase, L-lactate dehydrogenase, creatine kinase, GDP-L-fucose synthase, pyruvate kinase, fructose-bisphosphate aldolase, carbonic anhydrase, phosphopyruvate hydratase, phosphoglycerate kinase, *S*-(hydroxymethyl) glutathione dehydrogenase, and AMP deaminase. Real-time PCR assays showed that the level of mRNA expression of differentially expressed genes was positively correlated with growth. Proteins that were differentially expressed in GH exhibited fewer differences from GP and more differences from GE. These data are the first to reveal the molecular mechanism whereby growth is regulated in *G.* hybrid and its parents at the protein level. The study thus provides important information for genetic breeding and improvement of *G.* hybrid for aquaculture production.

Keywords: *Gymnocypris* hybrid; proteomics; metabolic changes; growth; *Gymnocypris przewalskii* ♀ × *G. eckloni* ♂

Key Contribution: The F_1 hybrid fish present heterosis in their growth and survival rates. This is the first report on proteomic analysis of hybrid *Gymnocypris*. TMT-based quantitative proteomics reveals the metabolic changes underlying the growth superiority of F_1 hybrid *Gymnocypris*.

check for updates

Citation: Dong, Y.; Zhou, J.; Xu, D.; Zhao, Y.; Qi, D. TMT-Based Quantitative Proteomics Reveal the Metabolic Changes Underlying Growth Superiority in a Novel *Gymnocypris* Hybrid, *Gymnocypris przewalskii* ♀ × *G. eckloni* ♂. *Fishes* **2024**, *9*, 158. https://doi.org/10.3390/fishes9050158

Academic Editor: Eric Hallerman

Received: 6 March 2024
Revised: 25 April 2024
Accepted: 26 April 2024
Published: 28 April 2024

1. Introduction

Gymnocypris przewalskii (GP), commonly known as "yellow carp", belongs to the Cypriniformes, Cyprinidae, Schizohoracinae, and Gymnocypi. Yellow carp is a cold-water, endemic fish species that evolved through long-term geographic isolation in Qinghai Lake, in which it is primarily distributed along affiliated rivers [1–3]. In Qinghai Lake, GP exhibits high adaptability, and after hatching, the fish swim in groups, generally gathering in shallow areas along river mouths. As the only dominant species in Qinghai Lake, GP occupies a central position in the lake's ecosystem [4]. *Gymnocypris eckloni* (GE), which also belongs to the Cypriniformes, Cyprinidae, Schizohoracinae, and Gymnocypri, is characterized by a dark-brown or bluish-gray back and a light-yellow or silver-gray underside [5,6]. In contrast to GP, GE is an economically important fish species found in the upper reaches of the Yellow River, and it is an omnivorous species with variable

feeding habits [7]. GE generally inhabits the middle layer of the water column and exhibits many characteristics similar to those of GP. The major difference is that GP's mouth gape is larger, and the upper jaw protrudes slightly relative to the lower jaw [8]. Due to significant environmental damage in recent years, fishery resources for these two *Gymnocypris* species have been depleted, and the number of wild populations has rapidly declined. In order to protect these fishery resources, we studied the novel species *Gymnocypris* interspecific hybrid (GH), generated by crossing *G. przewalskii* ♀ and *G. eckloni* ♂.

Hybridization not only enables the integration of excellent traits of both parent species, it also enables the generation of new traits not present in either parent, thus imparting various advantages to the hybrid offspring [9]. Interspecific hybridization is a useful strategy for achieving heterosis and thereby improving genotypic traits. Due to the combined effects of beneficial traits obtained from the male and female parents, hybrid varieties can exhibit heterosis in growth, survival, and disease resistance [10–13]. Most hybridization experiments currently conducted in fish involve crosses with different females, families, and genera, for example, *Clarias macrocephalus* ♀ × *C. gariepinus* ♂ [14], *Pseudoplatystoma reticulatum* × *Leiarius marmoratus* [15], *Carassius auratus cuvieri* ♀ × *Carassius auratus* red var. ♂ [16], *Heterobranchus longifilis* × *Clarias gariepinus* [17], and *Megalobrama amblycephala* ♀ × *Siniperca chuatsi* ♂ [18]. However, little information is available regarding GH, generated by crossing *G. przewalskii* ♀ × *G. eckloni* ♂, and no studies have reported the metabolic characteristics that underlie the growth superiority of GH.

Tandem Mass Tag (TMT) technology is an effective tool for overcoming the qualitative and quantitative problems associated with studying low-abundance proteins, and it has been widely applied in proteomics research [19]. TMT technology involves the specific labeling of the amino groups of peptides with 2, 6, or 10 isotopes, followed by tandem mass spectrometry analysis to simultaneously compare the relative contents of proteins in 2, 6, or 10 different samples [20]. The approach centers on first labeling proteins in different samples with different isotopic markers; the labeled proteins are then mixed before mass spectrometry analysis [21]. Thanks to its advantages, TMT technology is now widely used to analyze differentially expressed proteins (DEPs) in studies of metabolic changes in hybrid aquatic animals [22]. The primary factors that contribute to the metabolic changes underlying the growth superiority of novel GH have not been identified. In addition, to the best of our knowledge, no studies prior to the present study have examined the metabolic changes in GH using TMT technology.

Our study used GP as the female parent and GE as the male parent, and we report for the first time the metabolic changes that underlie the growth superiority of the F_1 progeny, GH. By comparing the proteomic profiles of GH and its parents, we discovered important information about metabolic changes that underlie the growth superiority of GH. The results of our research also provide a theoretical basis for the breeding of GH and a reference for the hybrid breeding and aquaculture practices involving other *Gymnocypris* species.

2. Materials and Methods

2.1. Experimental Animals

All experiments were carried out at the Xide Zhengyuan Fish Farm in Liangshan Prefecture, Sichuan Province, China. GP ♀, GE ♂, and F_1 GH were cultivated under the same breeding conditions. After hatching, the three types of *Gymnocypris* (500 of each *Gymnocypris* species or hybrid) were cultured in net cages in filtered water, with three biological replicates for each experimental group. Fish were cultivated for 6 months under the same conditions of temperature (13 °C) and light (on at 6:00 and off at 18:00); freshwater and food were maintained for 6 months. At the beginning and end of production, 15 fish were randomly taken for growth index measurement. Subsequently, three individuals from GH (length, 1.52 ± 0.07 cm), GP (length, 1.51 ± 0.06 cm), and GE (length, 1.53 ± 0.08 cm) were randomly selected for further experiments.

2.2. Sampling

Nine fish, each of GP, GE, and F1 GH, were randomly sampled, and the liver was quickly removed from each fish. The liver samples from each experimental group were mixed into one sample and stored at −80 °C for RNA extraction, proteomic analysis, and expression validation.

2.3. Protein Extraction and Determination

Liquid nitrogen was added to frozen tissue samples, which were then ground thoroughly and then transferred into a 1.5-mL centrifuge tube. Lysis solution, phosphatase inhibitor, and protease inhibitor were then added to each centrifuge tube to achieve a final concentration of 1 mM. The sample was then ground using a cold grinder at −35 °C at 60 Hz for 120 s, and then the operation was repeated. After grinding, the sample was centrifuged at 12,000 rpm and 4 °C for 10 min, and the supernatant was removed. The supernatant represented the total protein of the sample, and the concentration was measured using the BCA method (based on the oxidation-reduction reaction of proteins under alkaline conditions with bicinchonic acid). The protein solutions were stored at −80 °C until use.

2.4. Protease Hydrolysis, Peptide Labeling, and High-Performance Liquid-Phase Separation

Based on the measured protein concentrate 50 μg samples (3 samples for each experimental group) were taken. Different groups of samples were diluted to the same concentration and volume using lysis buffer [8 M urea and 40 mM Tris-HCl or triethylammonium bicarbonate (TEAB; pH 8.5)] to obtain protein. Dithiothreitol was added to the above protein solution to achieve a final concentration of 5 mM, and the sample was mixed well and incubated at 55 °C for 30 min, then cooled on ice to room temperature. An appropriate volume of iodoacetamide was added to achieve a final concentration of 10 mM, and the sample was mixed well and left at room temperature in the dark for 15 min. Six times the volume of acetone was then added to the sample, which was allowed to stand at −20 °C for >4 h. The sample was then centrifuged at 8000× *g* for 10 min and 4 °C, and the precipitate was collected. Add 100 μL TEAB (triethylammonium bicarbonate) after volatilizing acetone for 2–3 min. The precipitate was dissolved in TEAB (200 mM), and then 1 mg/mL trypsin TPCK(tosyl-phenylalanine chloromethyl-ketone) was added at a 1/50 sample-to-mass ratio, and the sample was digested overnight at 37 °C. After enzymatic hydrolysis, the sample was freeze-dried using a freeze-drying apparatus. Next, 100 mM TEAB buffer was added to the freeze-dried sample, which was shaken well and then labeled in a 1.5-mL Eppendorf tube. The Tandem Mass Tag (TMT) labeling reagent was removed from the refrigerator, equilibrated to room temperature, and then redissolved by the addition of anhydrous acetonitrile, followed by mixing and centrifugation. TMT reagent was then added to the sample, shaken to mix well, and then allowed to stand at room temperature for 1 h. Finally, 5% hydroxylamine was added to terminate the reaction, and the sample was freeze-dried and stored at −80 °C.

Sample components were separated by liquid chromatography (Agilent 1100 HPLC) using an Agilent Zorbax Extend-C18 narrow-bore column (2.1 × 150 mm, 5 μm).

2.5. Liquid Chromatography–Mass Spectrometry Analysis

Each component was loaded onto the EASY-nLC 1200 liquid-phase system (Thermo Fisher) at a 300 nL/min flow rate for separation. Mobile phase A consisted of ACN-H_2O-FA (99.9:0.1, *v*/*v*), and mobile phase B consisted of ACN-H_2O-FA (80:19.9:0.1, *v*/*v*/*v*). Gradient elution conditions were as follows: 0–50 min, 2–28% B; 50–60 min, 28–42% B; 60–65 min, 42–90% B; 65~75 min, 90% B. The peptide segments were separated using an ultra-high-performance liquid chromatography system and injected into a Q Active HF mass spectrometer (Thermo Fisher) for analysis. The mass spectrometry conditions were as follows: the mass resolution of the first level MS was set to 60,000; the automatic gain control value was set to $3e_6$; and the maximum injection time was 50 ms. The mass

spectrometer was set to full scan over the mass-to-charge ratio (m/z) range of 350–1500, and MS/MS scanning was performed on the 20 highest-intensity peaks. All MS/MS spectra were collected using data-dependent, high-energy collision fragmentation in positive ion mode, with the collision energy set to 32. The MS/MS resolution was set to 45,000; the automatic gain control was set to $2e_5$; the maximum ion injection time was 80 ms; and the dynamic exclusion time was set to 30 s.

2.6. Qualitative, Quantitative, and Functional Analysis of Proteins

For spectral analysis, original mass spectrometry data were imported into Proteome Discoverer software (version 2.4, Thermo Fisher Scientific, Waltham, MA, USA). The mass spectrometry retrieval parameters included parent ion tolerance of 10 ppm, daughter ion tolerance of 0.02 Da, fixed modifications of TMT (N-term, K) and carbamidomethyl (C), and variable modifications of oxidation (M) and acetylation (N-term), with a maximum of 2 omission sites.

Proteins exhibiting $p < 0.05$ and fold-change > 1.2 were considered significantly up-regulated, and those exhibiting $p < 0.05$ and FC < 1/1.2 were considered significantly downregulated. The Gene Ontology (GO) database (http://www.geneontology.org/, accessed on 1 November 2023) was applied to analyze the biological process (BP), cellular component (CC), and molecular function (MF) characteristics of the differentially expressed proteins based on their biological functions and classifications. The major pathways associated with the DEPs were analyzed using the Kyoto Encyclopedia of Genes and Genomes (KEGG) database (http://www.genome.jp/kegg/, accessed on 1 November 2023). Differential protein-protein interaction analysis was performed based on the string database to construct a differential protein interaction network.

2.7. Quantitative Real-Time PCR (qRT-PCR) Analysis

Trizol reagent was employed to extract total RNA from liver samples according to the manufacturer's instructions. The integrity of the isolated RNA was assessed using 1% agarose gel electrophoresis. cDNA synthesis was performed using a PrimeScript® RT Reagent kit with gDNA Eraser (Takara Bio Inc., Shiga, Japan), and the resulting cDNAs served as the template for qRT-PCR analyses. The list of primers [We designed two complementary primers using SnapGene (version 7.0.2, GSL Biotech, Boston, MA, USA)] based on the known target DNA sequence used in this study is presented in Supplemental File: Table S1. SYBR®-Premix Ex Taq™ was utilized for qRT-PCR amplifications on an ABI7500 Real-Time PCR Detection System (Applied Biosystems, Waltham, MA, USA) with a 20 µL reaction mixture. Quantitative analysis of the expression of target genes in each sample was carried out according to the ($2^{-\Delta\Delta Ct}$) method. Each experiment included three biological duplicates.

2.8. Statistical Analyses

Data regarding the body length, weight, and survival rate of juvenile fish were collected and used to calculate the following parameters:

$$\text{Survival rate (\%)} = \text{Final number of fish}/\text{Initial number of fish}$$

$$\text{Weight-gain rate (\%)} = (\text{Terminal weight} - \text{Initial weight})/\text{Initial weight}$$

Microsoft Excel 2021 (Microsoft, Washington, DC, USA) and SPSS version 26.0 (SPSS, Chicago, IL, USA) were used for statistical analyses. Differences between the three groups were analyzed using the Student's *t*-test, whereas one-way ANOVA and Duncan's method were used to compare multiple means between the experimental groups. Before statistical analyses, data were tested for normality and homoscedasticity of variances. Differences were considered significant at $p < 0.05$, and data are expressed as mean ± standard deviation (SD).

3. Results

3.1. Growth Trait Analysis

Significant differences were observed in terms of final length and weight, survival rate, and weight gain rate ($p < 0.05$; Table 1). The indexes of final length and weight and weight gain rate showed a ranking of GE > GH > GP, whereas with regard to survival rate, the ranking changed to GH > GE > GP.

Table 1. Growth trait characteristics of F_1 hybrid *Gymnocypris* and its parents.

		***Gymnocypris* Hybrid (GH)**	***Gymnocypris przewalskii* ♀ (GP)**	***Gymnocypris eckloni* ♂ (GE)**
Length	initial	1.52 ± 0.07	1.51 ± 0.06	1.53 ± 0.08
	final	8.39 ± 0.18 ^{b}	7.40 ± 0.19 ^{c}	11.25 ± 0.25 ^{a}
Weight	initial	1.71 ± 0.08	1.74 ± 0.07	1.75 ± 0.07
	final	9.32 ± 0.25 ^{b}	5.43 ± 0.30 ^{c}	19.83 ± 0.53 ^{a}
Weight-gain rate (%)		445.86 ± 24.85 ^{b}	212.61 ± 22.24 ^{c}	1037.29 ± 44.67 ^{a}
Survival rate (%)		80.30 ± 0.80 ^{a}	65.20 ± 1.12 ^{c}	72.27 ± 0.74 ^{b}

Note: significant differences between treatments are indicated by different letters ($p < 0.05$).

3.2. Primary Data Analysis and Protein Detection

The TMT proteomics analysis generated a total of 374,786 spectra using the liver as a sample. A total of 12,151 peptides and 1784 proteins were detected from among 27,077 known spectra (Figure 1A). Most of the identified proteins were covered by no fewer than six peptides (Figure 1B), indicating that the identified proteins exhibited good sequence coverage. In terms of protein mass distribution, 64.74% of the total proteins were identified in the molecular weight groups 10–20 kD (110), 20–30 kD (142), 30–40 kD (141), 40–50 kD (168), 50–60 kD (195), 60–70 kD (169), 70–80 kD (124), and 80–90 kD (106) (Figure 1C). In terms of sequence coverage, 68% of the proteins exhibited 10% sequence coverage, and 32% exhibited >10% sequence coverage (Figure 1D).

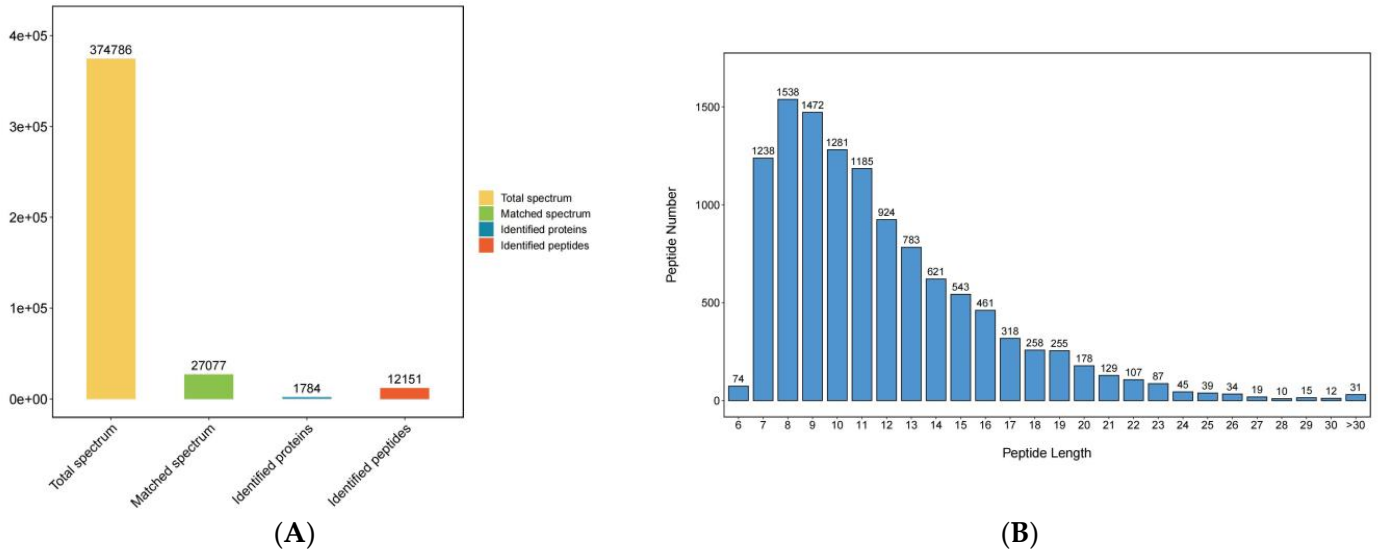

(**A**) (**B**)

Figure 1. *Cont.*

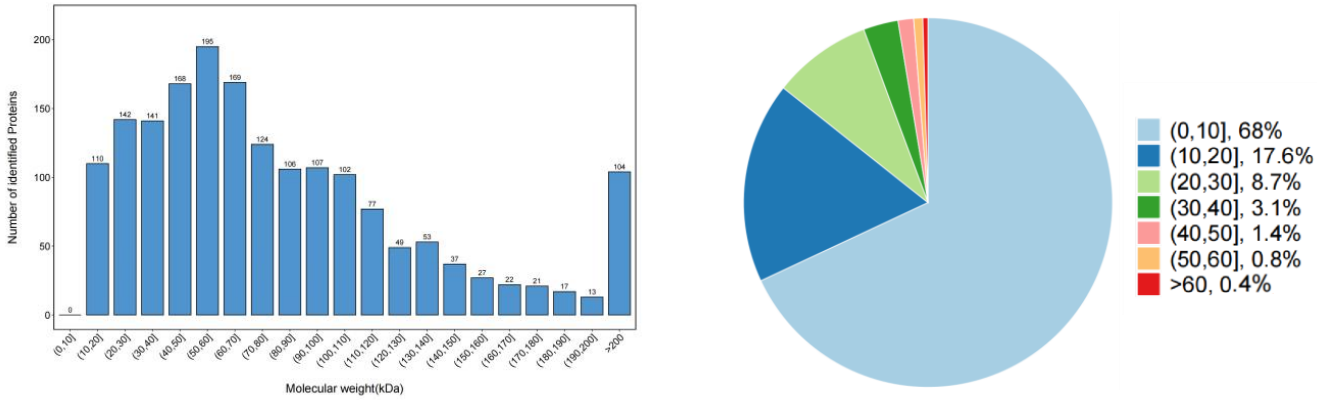

(**C**) (**D**)

Figure 1. (**A**) Basic statistics for TMT proteomics data. (**B**) Distribution of proteins associated with different quantities of recognized peptides. (**C**) Distribution of proteins in different molecular weight categories (kD). (**D**) Peptide coverage of identified proteins.

3.3. Identification and Comparison of DEPs

In order to compare the differences in liver proteomics between the GP, GE, and GH groups, a volcano plot was drawn based on *p*-value (−log10 *p*-value) and log2 fold-change in the expression of each protein. The results showed that the proportion of proteins in the GP group (Figure 2A) and GE group (Figure 2B) changed compared with GH. Hierarchical clustering heatmaps of the two sets of DEPs are shown in Figure 3, and cluster analysis also indicated that similar samples exhibited similar distances and preferentially clustered.

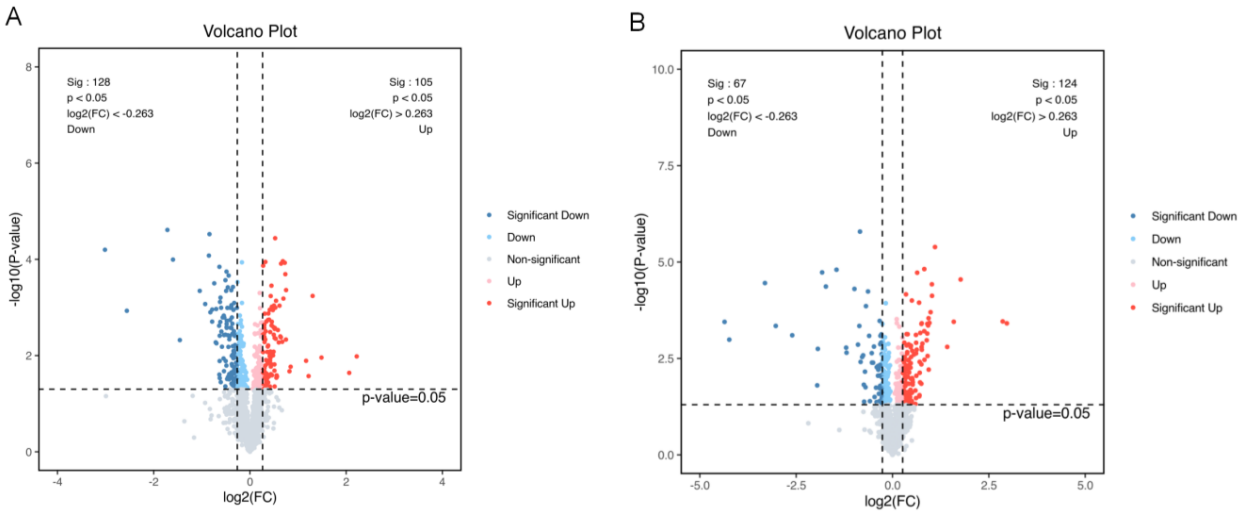

Figure 2. Volcano plot showing differentially expressed proteins in liver samples. (**A**) Comparison between the GP group and GH group. (**B**) Comparison between the GE group and GH group. Points highlighted in red (change factor FC > 1.2) and blue (FC < 0.83) indicate significant changes in protein levels ($p < 0.05$).

The expression levels of 197 proteins in GE vs. GH comparison showed significant changes, with 124 upregulated proteins (64.92%) and 67 down-regulated proteins (35.08%) (Figure 4A). In the amino acid metabolism pathway, HRE (K00049, FC = 1.36) was up-regulated, and aldehyde dehydrogenase (K14085, FC = 0.80) and AHE (K01251, FC = 0.79) were down-regulated. In terms of carbohydrate metabolism, GDP–L-fucose synthase (K02377, FC = 1.68) was upregulated, and fructose-bisphosphate aldolase (FAE) (K01623, FC = 0.12) was down-regulated. In terms of energy metabolism, carbonic anhydrase (CAE) (K18245, FC = 1.68) and four cytochrome C oxidases (K02272, K02270, K02265, and K02263,

FC = 1.25, 1.22, 1.24, and 1.77, respectively) were upregulated. Dolichyl-phosphate beta-glucosyltransferase (K00729, FC = 1.39) was upregulated regarding glycan biosynthesis and metabolism. An uncharacterized protein (K16342, FC = 0.16) was down-regulated in lipid metabolism. Finally, regarding xenobiotic biodegradation and metabolism, myeloid-specific peroxidase (K10789, FC = 0.78) was down-regulated (Table 2).

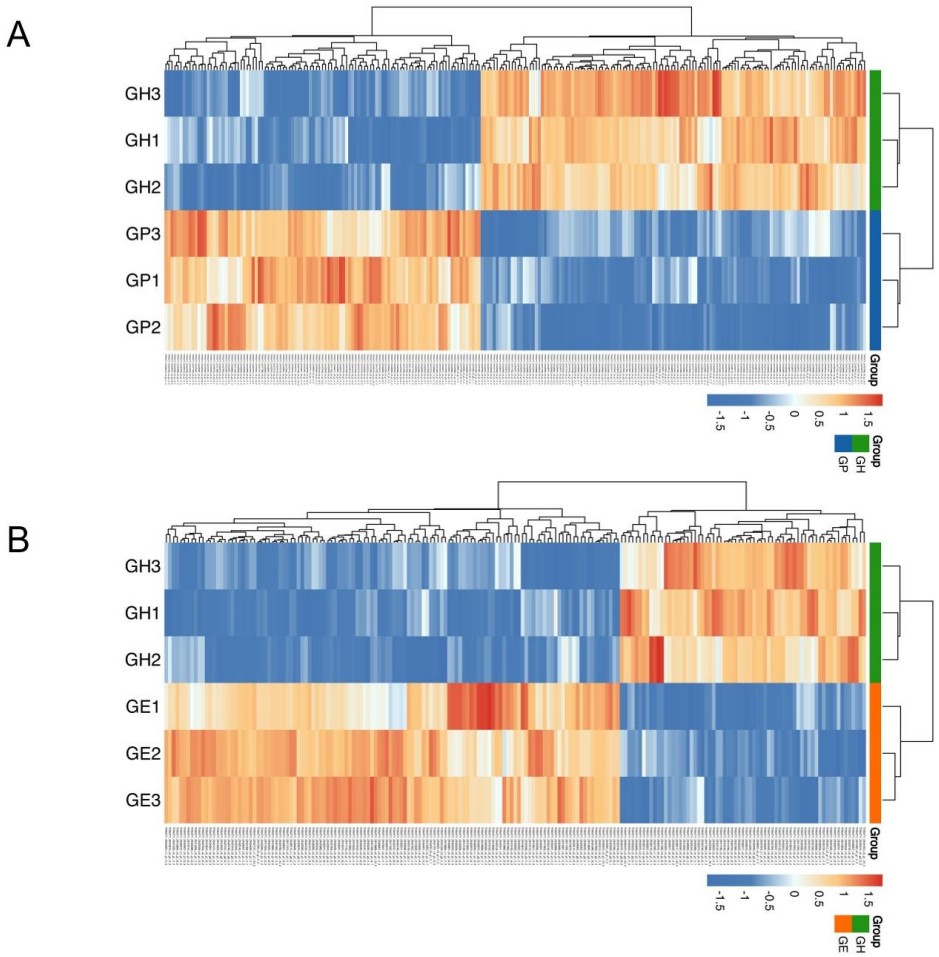

Figure 3. Cluster analysis of liver samples. (**A**) Comparison between the GP group and GH group. (**B**) Comparison between the GE group and GH group. Different colors represent different relative protein abundance, red representing high intensity, and blue representing low intensity.

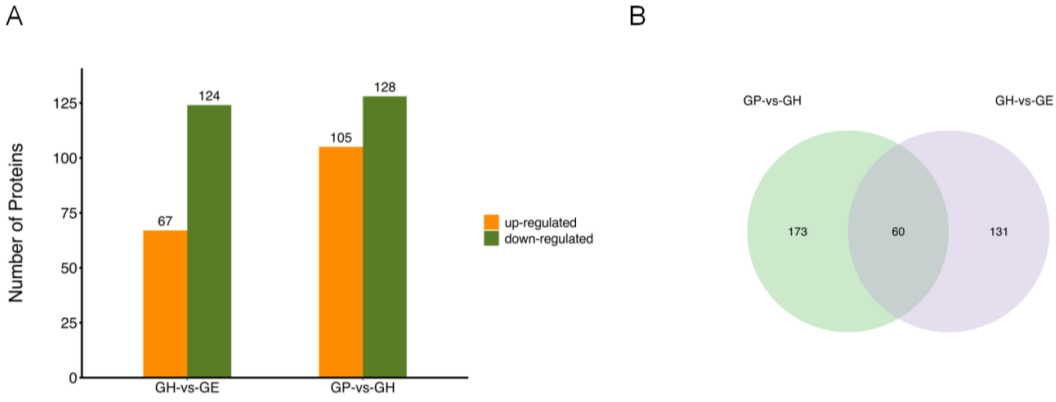

Figure 4. Distribution of differentially expressed proteins in the liver. (**A**) Number of differentially expressed proteins (GH vs. GE and GP vs. GH) (multiple difference > 1.2 or <0.83; p value < 0.05). (**B**) Venn diagram of differentially expressed proteins (GP vs. GH and GH vs. GE).

Table 2. Metabolism-related DEPs identified in the liver (GE vs. GH and GP vs. GH).

Accession	Protein Name	Coverage [a]	Peptides [b]	Score [c]	Fold Change [d] (GE-GH)	Fold Change [d] (GP-GH)
Amino acid metabolism						
K14085	Aldehyde dehydrogenase (NAD (+))	28	14	121.38	0.80	-
K00049	Hydroxypyruvate reductase	8	3	13.6	1.36	-
K01251	Adenosylhomocysteinase	27	17	127.11	0.79	-
K01756	Adenylosuccinate lyase	24	17	103.56	-	0.77
K01939	Adenylosuccinate synthetase isozyme 1	31	21	190.49	-	0.72
K11204	Glutamate--cysteine ligase	2	2	5.26	-	1.23
K00016	L-lactate dehydrogenase	25	14	188.87	-	0.79
K00933	Creatine kinase	30	19	370.61	-	0.82
K01834	Phosphoglycerate mutase	44	20	310.04	-	0.65
K11426	N-lysine methyltransferase SMYD2-B-like	16	8	42.65	-	0.71
K15791	Dehydrogenase E1 and transketolase domain containing 1	12	10	47.04	-	0.78
Carbohydrate metabolism						
K01623	Fructose-bisphosphate aldolase	6	1	9.65	0.12	0.66
K02377	GDP-L-fucose synthase	14	7	19.32	1.68	-
K00873	Pyruvate kinase	31	31	703.85	-	0.68
K01835	Phosphoglucomutase-1-like	39	26	362.7	-	0.70
K01057	6-phosphogluconolactonase	20	5	19.89	-	0.74
K00850	ATP-dependent 6-phosphofructokinase	27	28	249.79	-	0.69
K01176	Alpha-amylase	9	1	3.64	-	0.81
K00688	Alpha-1,4 glucan phosphorylase	37	54	1155.49	-	0.69
K19029	6-phosphofructo-2-kinase domain-containing protein	1	1	3.05	-	0.70
K01578	Malonyl-CoA decarboxylase	3	2	6.18	-	1.21
K21797	SAC domain-containing protein	1	1	3.68	-	1.23
Energy metabolism						
K02272	Cytochrome c oxidase subunit 7C, Mitochondrial	7	1	6.46	1.25	-
K02270	Cytochrome c oxidase subunit 7A2, Mitochondrial-like	3	1	7.86	1.22	-
K02265	Cytochrome c oxidase subunit 5B, Mitochondrial-like	22	6	37.84	1.24	-
K02263	Cytochrome c oxidase subunit 4I2	20	9	44.86	1.77	-
K18245	Carbonic anhydrase	20	9	65.21	1.68	-
K01689	Phosphopyruvate hydratase	21	10	361.35	-	0.62
K00134	Glyceraldehyde-3-phosphate dehydrogenase (phosphorylating)	61	22	940.86	-	0.62
K00927	Phosphoglycerate kinase	45	24	393.87	-	0.66
K03949	NADH dehydrogenase [ubiquinone] 1 Alpha subcomplex subunit 5	13	1	17	-	1.33
K02267	Cytochrome c oxidase subunit	19	3	34.29	-	0.83
K00237	Succinate dehydrogenase [ubiquinone] cytochrome b small subunit	2	1	5.76	-	1.23
K03953	NADH dehydrogenase [ubiquinone] 1 alpha subcomplex subunit 9, Mitochondrial-like	10	6	28.92	-	1.29
K22470	FAD/NAD(P)-binding domain-containing protein	22	13	55.06	-	1.36
Glycan biosynthesis and metabolism						
K00729	Dolichyl-phosphate beta-glucosyltransferase	1	1	3.22	1.39	0.72
Lipid metabolism						
K16342	Uncharacterized protein	9	5	19.35	0.16	2.80
K01897	AMP-dependent synthetase/ligase domain-containing protein	4	4	11.13	-	0.65
K00121	S-(hydroxymethyl)glutathione dehydrogenase	22	8	43.62	-	0.80
K15717	Prostamide/prostaglandin F synthase	8	3	26.89	-	1.41

Table 2. *Cont.*

Accession	Protein Name	Coverage [a]	Peptides [b]	Score [c]	Fold Change [d] (GE-GH)	Fold Change [d] (GP-GH)
Metabolism of cofactors and vitamins						
K00214	Biliverdin reductase A-like	13	4	22.97	-	1.27
Xenobiotics biodegradation and metabolism						
K10789	Myeloid-specific peroxidase	1	1	2.68	0.78	-
K01061	Carboxymethylenebutenolidase homolog	10	3	12.87	-	0.77
Nucleotide metabolism						
K00939	Adenylate kinase isoenzyme 1	19	17	342.16	-	0.78
K01490	AMP deaminase	4	5	59.44	-	0.76
K13421	Uridine 5′-monophosphate synthase	7	4	12.6	-	1.24

Note: [a] Coverage indicates the coverage of protein sequence. [b] Peptide indicates peptide sequence number matching a protein. [c] Score indicates identification score of proteins. [d] The values were calculated as the ratio (GE-vs-GH and GP-vs-GH).

The expression levels of 233 proteins in the GP vs. GH comparison showed significant changes, with 105 upregulated proteins (45.06%) and 128 down-regulated proteins (54.94%) (Figure 4A). With regard to amino acid metabolism, glutamate-cysteine ligase (GCE) (K11204, FC = 1.23) was upregulated, and three proteins exhibiting the highest fold down-regulation included phosphoglycerate mutase (K01834, FC = 0.65), N-lysine methyltransferase (K11426, FC = 0.71), and adenylosuccinate synthetase isozyme (K01939, FC = 0.72). Regarding carbohydrate metabolism, malonyl-CoA decarboxylase (K0578, FC = 1.21) and SAC domain-containing protein (K21797, FC = 1.23) were upregulated, and four proteins with the highest fold down-regulation included FAE (K01623, FC = 0.66), pyruvate kinase (PKE) (K00873, FC = 0.68), alpha-1,4 glucan phosphorylase (K00688, FC = 0.69), and ATP-dependent 6-phosphofructokinase (K00850, FC = 0.69). Regarding lipid metabolism, three proteins with the highest fold up-regulation included NADH dehydrogenase (K03949 and K03953, FC = 1.33 and 1.29), FAD/NAD(P)-binding domain-containing protein (K22470, FC = 1.36), and phosphopyruvate hydratase (PHE) (K01869, FC = 0.62). Glyceraldehyde-3-phosphate dehydrogenase (K00134, FC = 0.62) and phosphoglycerate kinase (K00927, FC = 0.16) were down-regulated. Regarding glycan biosynthesis and metabolism, dolichyl-phosphate beta-glucosyltransferase (K00729, FC = 0.72) was down-regulated. Regarding lipid metabolism, an uncharacterized protein (K16342, FC = 2.80) and prostaglandin F synthase (K15717, FC = 1.41) were up-regulated, and AMP-dependent synthetase (K01879, FC = 0.65) and S-(hydroxymethyl) glutathione dehydrogenase (SDE) (K00121, FC = 0.80) were down-regulated. Regarding xenobiotic biodegradation and metabolism, carboxymethylenebutenolidase homolog (K01061, FC = 0.77) was down-regulated. Regarding nucleotide metabolism, uridine 5′-monophosphate synthase (K13421, FC = 1.24) was upregulated, and adenylate kinase isoenzyme (K00938, FC = 0.78) and AMP deaminase (ADE) (K01490, FC = 0.76) were down-regulated (Table 2).

A total of 60 common DEPs were identified (GE vs. GH and GP vs. GH) (Figure 4B) and included FAE (K01623, FC = 0.12), dolichyl-phosphate beta-glucosyltransferase (K00729, FC = 1.39), and an uncharacterized protein (K16342, FC = 0.16) involved in cellular metabolism.

3.4. GO Pathway Enrichment Analysis of DEPs

GO Slim classification was used to classify all proteins, and the result highlighted the enrichment characteristics of specific functional categories in different groups (GH vs. GE and GP vs. GH). According to GO terminology, DEPs can be classified into three functional categories: BP (Biological Process), CC (Cellular Component), and MF (Molecular Function).

In the BP category (22 processes), DEPs were primarily involved in biological adhesion, biological regulation, cell killing, cellular component organization or biogenesis, cellular processes, developmental processes, establishment of localization, growth, immune system processes, localization, locomotion, metabolic processes, muti-organism processes, multicel-

lular organismal processes, regulation of biological processes, reproduction processes, and response to stimuli. In the CC category (20 processes), DEPs were primarily related to the cell, extracellular matrix, extracellular region, macromolecular complex, membrane, and organelles. In the MF category (21 processes), the DEPs were primarily related to antioxidant activity, binding, catalytic activity, enzyme regulatory activity, structural molecular activity, translation regulator activity, and transporter activity (Figure 5).

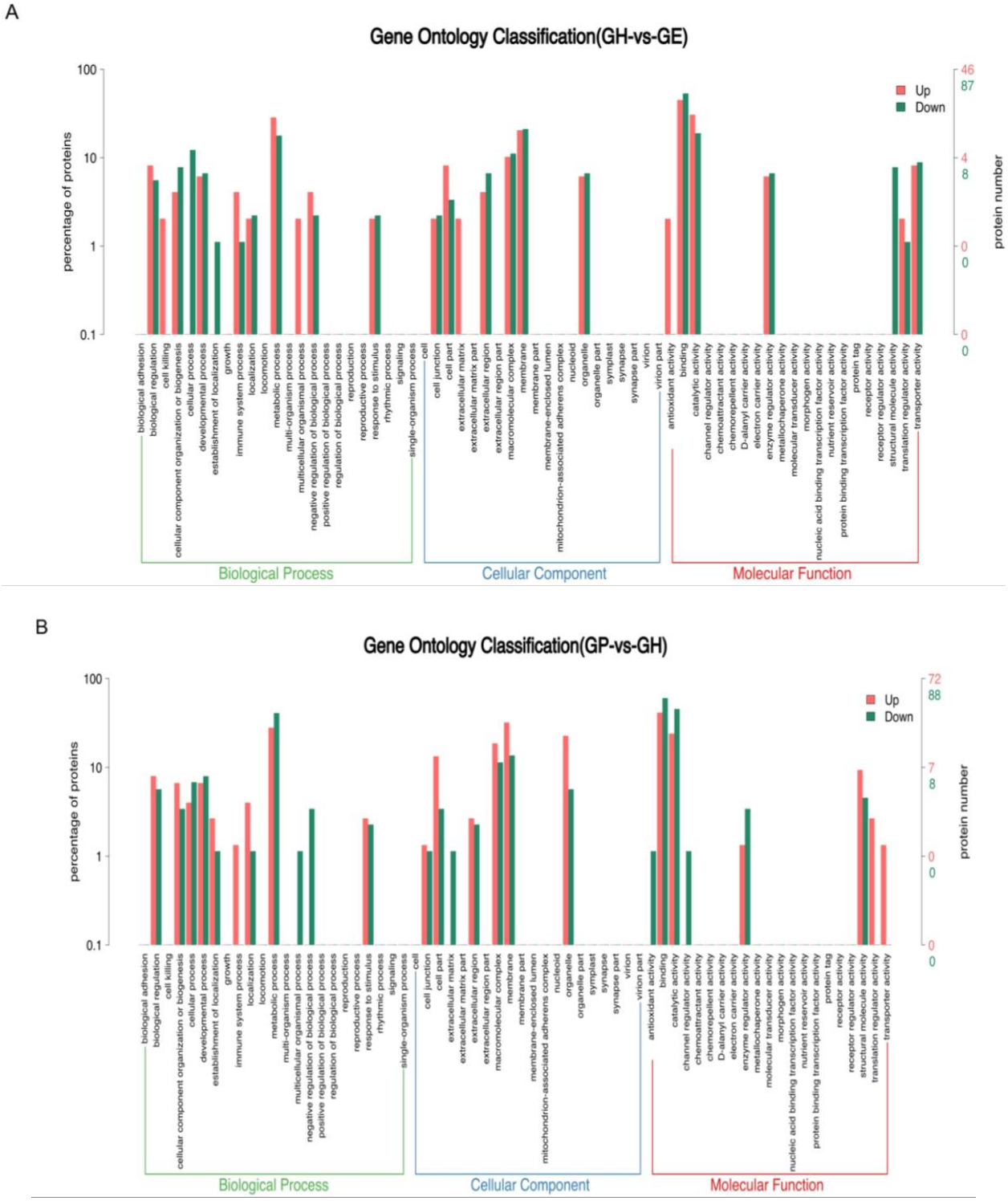

Figure 5. Gene Ontology (GO) classification of DEPs in liver samples in GH vs. GE (**A**) and GP vs. GH (**B**) comparisons.

3.5. KEGG Pathway Analysis of the Relationship between DEPs and Metabolism

The metabolic pathways associated with DEPs were classified using the KEGG database. All DEPs were classified into five categories based on their biological function, including metabolism (GH vs. GE: 20 DEPs; GP vs. GH: 63 DEPs), cellular processes (GH vs. GE: 36 DEPs; GP vs. GH: 34 DEPs), genetic information processing (GH vs. GE: 9 DEPs; GP vs. GH: 13 DEPs), environmental information processing (GH vs. GE: 11 DEPs; GP vs. GH: 14 DEPs), and organismal systems (GH vs. GE: 54 DEPs; GP vs. GH: 69 DEPs) (Figure 6A,B).

Pathways related to metabolism were further subdivided into eight subgroups (Level 2): xenobiotic biodegradation and metabolism (GH vs. GE: 1 DEP; GP vs. GH: 3 DEPs), metabolism of other amino acids (GH vs. GE: 1 DEP; GP vs. GH: 2 DEPs), metabolism of cofactors and vitamins (GH vs. GE: 1 DEP; GP vs. GH: 4 DEPs), lipid metabolism (GH vs. GE: 2 DEPs; GP vs. GH: 4 DEPs), glycan biosynthesis and metabolism (GH vs. GE: 2 DEPs; GP vs. GH: 1 DEP), energy metabolism (GH vs. GE: 6 DEPs; GP vs. GH: 13 DEPs), carbohydrate metabolism (GH vs. GE: 4 DEPs; GP vs. GH: 18 DEPs), amino acid metabolism (GH vs. GE: 3 DEPs; GP vs. GH: 11 DEPs), nucleotide metabolism (GH vs. GE: 0 DEPs; GP vs. GH: 6 DEPs), and biosynthesis of other secondary metabolites (GH vs. GE: 0 DEPs; GP vs. GH: 1 DEP) (Figure 6A,B, Table 2).

The KEGG pathway enrichment analysis of DEPs in the GH vs. GE comparison detected 130 KEGG pathways (Figure 6A), with the first 20 showing significant changes ($p < 0.05$) (Figure 7A). In addition, we identified 4 KEGG pathways associated with metabolic products: fructose and mannose metabolism, pyruvate metabolism, estrogen signaling pathway, and oxidative phosphorylation.

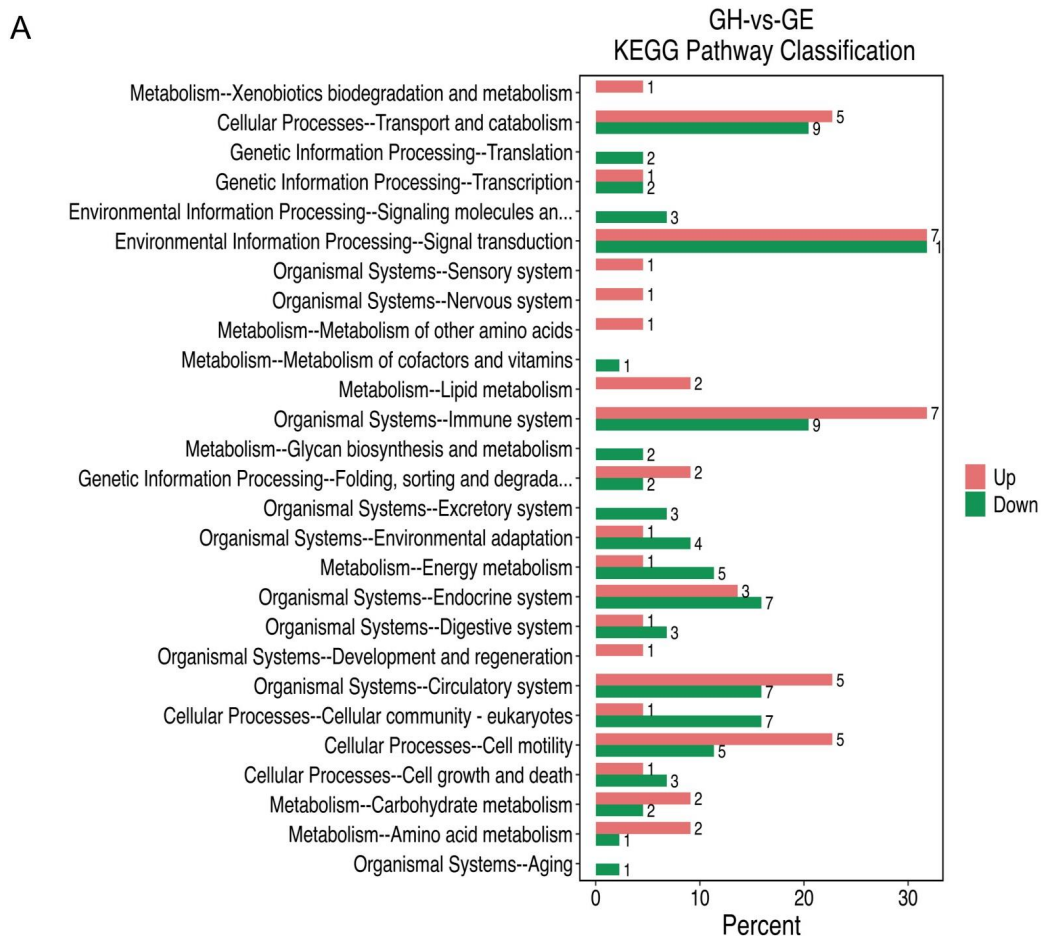

Figure 6. *Cont.*

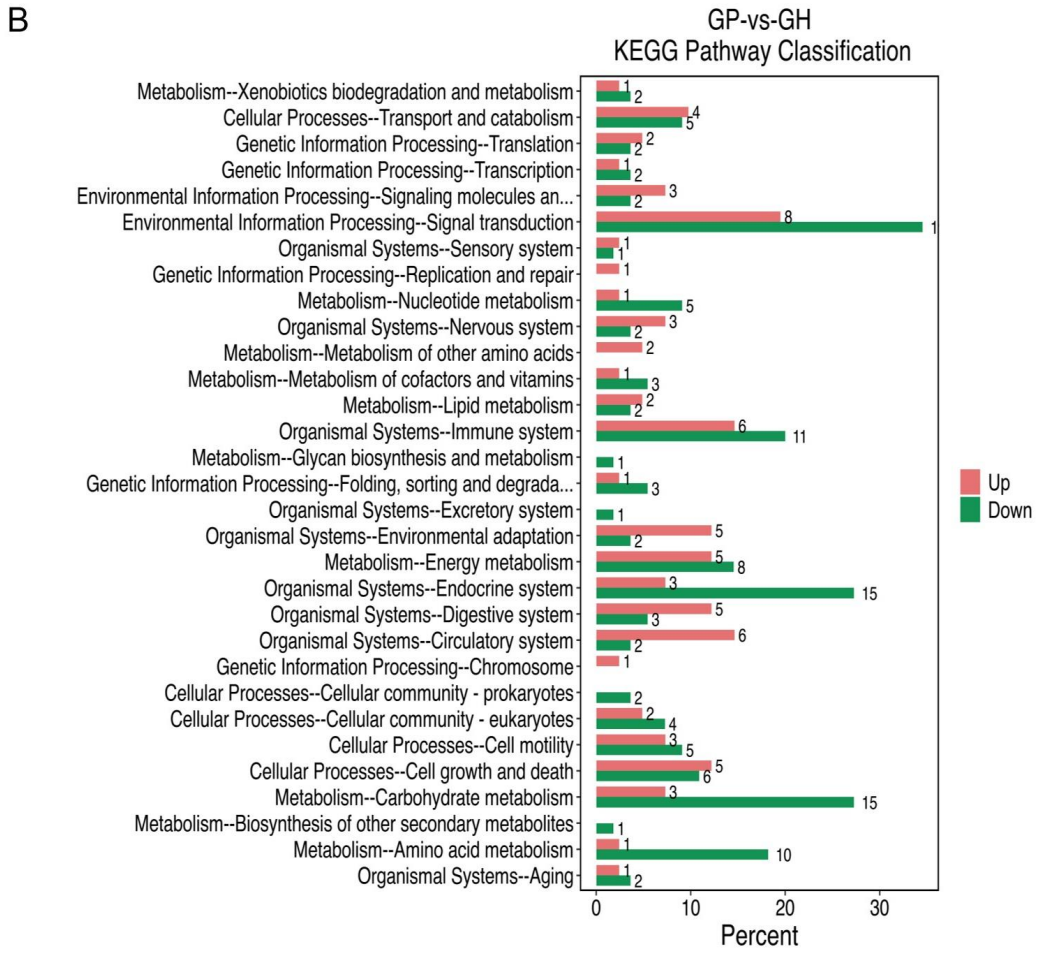

Figure 6. KEGG pathway classification analyses of DEPs in liver samples in the GH vs. GE (**A**) and GP vs. GH (**B**) comparisons.

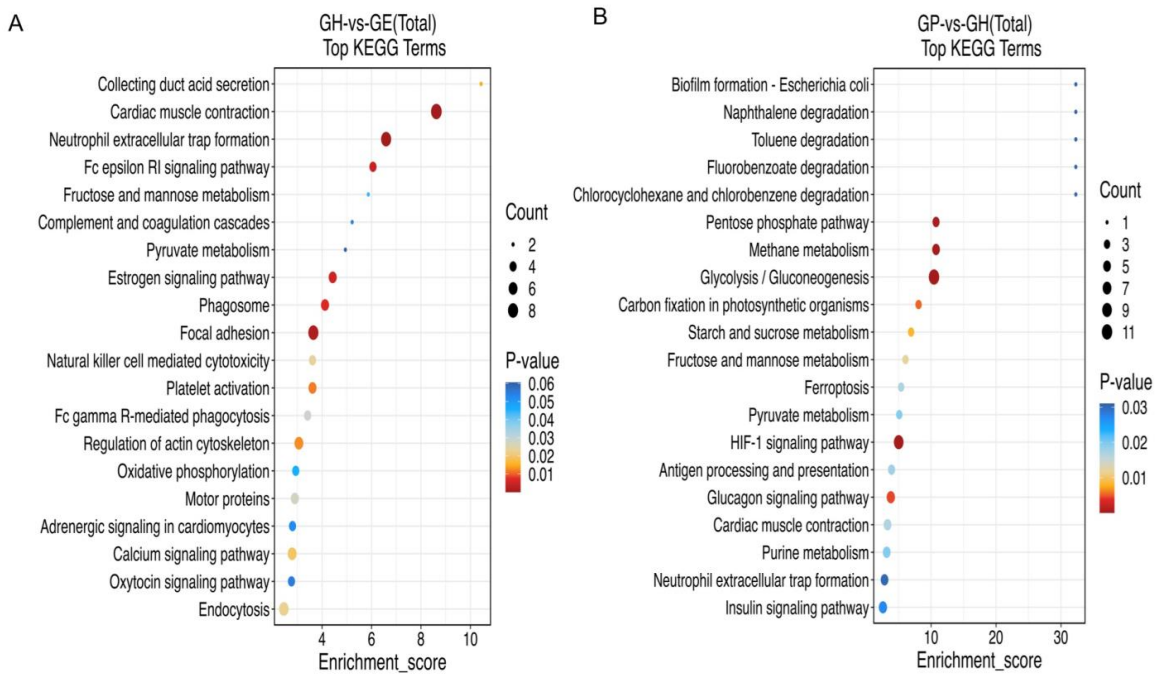

Figure 7. KEGG pathway enrichment analyses of DEPs in liver samples in the GH vs. GE (**A**) and GP vs. GH (**B**) comparisons.

KEGG pathway enrichment analysis of DEPs in the GP vs. GH comparison detected 205 KEGG pathways (Figure 6B). Among the top 20 pathways (Figure 7B), 9 are directly related to metabolism: pentose phosphate pathway, methane metabolism, glycolysis (gluconeogenesis), starch and sucrose metabolism, fructose and mannose metabolism, pyruvate metabolism, glucagon signaling pathway, purine metabolism, and insulin signaling pathway.

3.6. qRT-PCR Validation of Proteomic Data

The mRNA transcription levels of the genes encoding 11 identified DEPs (CA2, carbonic anhydrase 2; COX4, cytochrome c oxidase subunit 4; ALG5, dolichyl-phosphate beta-glucosyltransferase; ALDH7A1, aldehyde dehydrogenase family 7 member A1; ALDO, fructose-bisphosphate aldolase, class I; AHCY, adenosylhomocysteinase; PGLS, 6-phosphogluconolactonase; PK, pyruvate kinase; PGK, phosphoglycerate kinase; COX6A, cytochrome c oxidase subunit 6a; and SQOR, eukaryotic sulfide quinone oxidoreductase) were determined using qRT-PCR to validate the TMT results. As shown in the qRT-PCR results for 12 randomly selected genes, the transcripts exhibited expression changes similar to the TMT results (Figure 8). Overall, the qRT-PCR data were consistent with the proteomic analysis data obtained using the TMT approach, demonstrating the reliability of the TMT proteomic method.

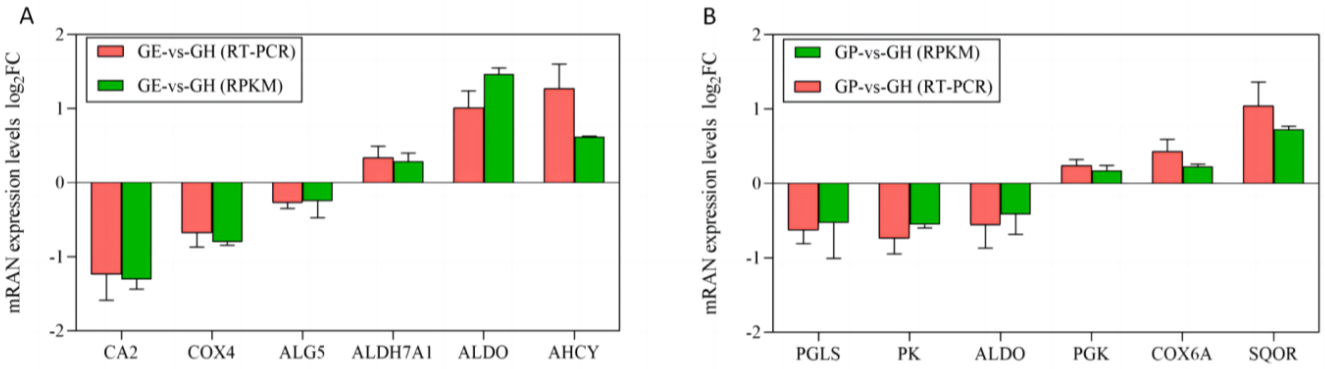

Figure 8. Quantitative real-time PCR (qRT-PCR) analysis of the expression of genes encoding DEPs in GE vs. GH (**A**) and GP vs. GH (**B**).

Note:Proteins are abbreviated as follow:ALDO, fructose-bisphosphate aldolase, class I; PK, pyruvate kinase; PGLS, 6-phosphogluconolactonase; PGK, phosphoglycerate kinase; COX6A, cytochrome c oxidase subunit 6a; SQOR, eukaryotic sulfide quinone oxidoreductase; COX4, cytochrome c oxidase subunit 4; CA2, carbonic anhydrase 2; ALG5, dolichyl-phosphate beta-glucosyltransferase; ALDH7A1, aldehyde dehydrogenase family 7 member A1; AHCY, adenosylhomocysteinase.

4. Discussion

Hybrid production is an effective approach to generate better varieties and prevent variety degradation [23]. Hybrids often exhibit heterosis in terms of growth rate, survival rate, and disease resistance [24]. Among vertebrates, fishes exhibit a variety of unique characteristics that render them suitable for hybridization [25]. Therefore, hybrid production is very important for improving fish varieties and cultivating new ones. For example, the groupers *Epinephelus akaara* and *E. tukula* can undergo hybrid breeding with different species, genera, and subfamilies, resulting in a large number of hybrid offspring [26]. Hybrid species cultivated by crossbreeding of the basses *Morone chrysops* and *M. saxatilis* exhibit clear hybrid advantages, grow faster than the parents, and are more resistant to stress and disease than the parents [27]. In the hybridization of the catfishes *Ictalurus frucatus* and *I. punctatus*, the growth rate of the hybrid is >30% higher than that of the parents and thus exhibits obvious hybrid advantages [28]. In this study, we found that the growth rate of GP♀was significantly slower than that of GE♂, and the resulting GH

progeny clearly inherited the growth rate advantage of GE♂, which is significantly higher than that of GP♀but still lower than that of GE♂. It is possible that further backcrossing would improve the growth advantage of the hybrid species [29]. We also found that the survival rate of GH was significantly higher than that of its parents after 6 months, perhaps due to the GH expressing heterosis, stronger adaptability to environmental changes, and resistance to stress.

Recent studies have examined the relationship between parameters analyzed using omics approaches and the growth advantage of aquatic animals [30]. For example, a study of the protein expression profile of Pacific oyster *Crassostrea gigas* parents and hybrid offspring revealed that the biological metabolism of proteins plays an important role in the growth advantage of hybrid offspring [31]. In the present study, GH inherited the growth advantage of the GE♂parent. Growth advantage refers to the ability of an organism to exhibit better growth life under certain conditions compared with other stocks of the same species. This advantage can result from multiple factors, including environmental characteristics, genetics, physiology, and behavior, all of which are closely related to biological metabolism. Previously, we conducted a transcriptome analysis that revealed the molecular mechanisms underlying growth superiority in a novel hybrid *Gymnocypris*, GP♀× GE♂and found that many metabolism-related genes are associated with growth [32]. Based on these data, we plan to continue studying the relationship between the proteome and metabolism in these fish.

4.1. DEPs Related to Amino Acid Metabolism

The first step in the metabolism of proteins ingested by fish in their food, as well as the proteins that make up the body's cells and the proteins synthesized within cells, is the addition of water with the participation of various enzymes [33]. The GE vs. GH comparison results in the present study revealed 3 DEPs related to amino acid metabolism, two of which were significantly down-regulated and one significantly upregulated. AHE was found to be significantly down-regulated in the GE vs. GH comparison. The activity of AHE in vivo is directly related to the level of homocysteine in the blood. When AHE deficiency occurs, plasma levels of creatine kinase (CKE) and methionine increase, leading to developmental delay [34]. Some proteomic studies have found that acute crowding can increase AHE protein expression in rainbow trout *Oncorhynchus mykiss* [35]. However, the expression of AHE in GE ♂ was significantly reduced compared with GH, indicating that GH is more adaptable to changes in biotic and abiotic stress and accelerates its growth by regulating AHE activity. HRE, which catalyzes the formation of hydroxypyruvate from D-glycerate in the presence of NAD $(P)^+$, is involved in the metabolism of energy and substances in vivo [36]. Other studies have found that HRE promotes plant photorespiration and photosynthesis [37,38], but there have been no reports on HRE in aquatic animals. In the present study, HRE was significantly upregulated in the GE vs. GH comparison, indicating that in contrast to GE♂, GH may reduce energy losses and respond to adverse environmental conditions by reducing HRE activity.

Many DEPs related to amino acid metabolism were identified in the GP vs. GH comparison, indicating that amino acids are an important source of energy for both GP ♀ and GH. GCE is a rate-limiting enzyme in the glutathione biosynthesis pathway. GCE activity typically determines cellular glutathione levels and glutathione biosynthesis capacity. The enzyme also plays an important role in protein metabolism and participates in many important biochemical reactions [39]. Research has found that reduced GCE activity eliminates the response of the model plant *Arabidopsis thaliana* to changes in the redox environment [40]. In the present study, GCE was significantly upregulated in the GP vs. GH comparison, indicating that GH responds to changes in the redox environment by reducing GCE activity. L-lactate dehydrogenase (LDE) is a key enzyme in the glycolytic pathway and tricarboxylic acid cycle, and its activity can indicate anaerobic metabolism [41]. Another study found that the green mud crab *Scylla paramamosain* exhibits increased LDE activity and upregulates anaerobic pathways in low-salinity environments [42]. In the

present study, LDE was significantly down-regulated in the GP vs. GH comparison, indicating that GH reduces anaerobic respiration and allocates more energy toward growth than GP ♀. CKE is an important enzyme directly related to intracellular energy exchange, muscle contraction, and ATP regeneration, and it is mainly present in the cytoplasm and mitochondria [43]. Another study found that adding different proportions of creatine to spotted sea bass *Lateolabrax maculatus* feed affects the level of CKE [44]. In the present study, CKE was significantly down-regulated in the GP vs. GH comparison, indicating that GH reduces muscle contraction and stores energy in order to accelerate growth.

4.2. DEPs Related to Carbohydrate Metabolism

Carbohydrate metabolism is one of the most important metabolic processes, as it provides energy for basic biological activities and serves as the main form of energy storage in animals. In fishes, the primary organ for carbohydrate metabolism is the liver, which is also the primary organ for maintaining blood sugar balance. In this study, GDP–L-fucose synthase (GFE) was significantly upregulated in the GE vs. GH comparison. GFE is a lysosomal acidic hydrolase that catalyzes the hydrolysis of bioactive macromolecules such as glycoproteins and glycolipids containing fucose groups. GFE is widely distributed in tissue cells, blood, and body fluids and functions in the metabolism of glycoproteins, glycolipids, and oligosaccharides [45]. The significant up-regulation of GFE in the present study indicates that the disease resistance of GE ♂ weaker than that of GH, which may explain the low survival rate of GE ♂. PKE is a major enzyme involved in carbohydrate metabolism and plays an important allosteric role in glycolysis [46]. Another study found that in green mud crab *S. paramamosain*, PKE activity is increased and metabolism more vigorous under low-salinity conditions [47]. In the present study, the expression of PKE was down-regulated in the GP vs. GH comparison, thus promoting the generation of pyruvate in GH. Pyruvate is converted to acetyl CoA, which then enters the fatty acid biosynthesis pathway.

We noted that FAE was significantly down-regulated in both the GP vs. GH and GE vs. GH comparisons. FAE is an important enzyme involved in the Calvin cycle in glycolysis, gluconeogenesis, the pentose phosphate pathway, and photosynthesis. FAE is ubiquitous in animals and exhibits different responses under various stress conditions [48]. Previous proteomic studies found that acute crowding can increase FAE protein expression in rainbow trout *O. mykiss* [35] and also described changes in FAE expression in transgenic masu salmon *O. masou ishikawae* [49]. These results also indicate that GH's carbohydrate metabolism is more stable under various stress conditions than GP ♀ and GE ♂.

4.3. DEPs Related to Energy Metabolism

Energy metabolism is one of the most fundamental characteristics of living organisms [50] and usually involves the release, transfer, storage, and utilization of energy in the process of material metabolism. Most DEPs related to energy metabolism in the GE vs. GH comparison were significantly upregulated. CAE is the most important zinc-containing enzyme and functions in various ion exchange reactions and the maintenance of internal homeostasis. CAE's properties, structure, and distribution are related to various epithelial cells and bicarbonate salts. Previous studies have shown that high-salinity domestication does not significantly inhibit the CAE activity of *Carcinus maenas*, but low-salinity domestication has a significant inhibitory effect [51]. In the present study, the expression of CAE in the GE vs. GH comparison was upregulated. This up-regulation could have been related to the poor salinity tolerance of GE♂, whereas GH inherited the adaptive salinity mechanism of the maternal GP ♀.

The significantly down-regulated proteins in the present study included phosphopyruvate hydratase (PHE) and phosphoglycerate kinase (PTE) in the GP vs. GH comparison. PHE is a key enzyme in the sugar metabolism pathway and is expressed in large quantities, primarily in the cytoplasm of the cells of many organs. PHE converts 2-phosphoglycerate into phosphoenolpyruvate. This reaction is a key step in the glycolysis process. Some

studies have shown that PHE is highly expressed in the Japanese tiger prawn *Marsupenaeus japonicus* infected with *Schistosoma* [52]. Our research also indirectly indicates that GH exhibits greater disease resistance, which may be the reason for the higher survival rate of GH compared with GP♀. PTE is involved in energy production during carbon metabolism, catalyzing the high-energy phosphoryl transfer of acylphosphate from 1,3-diphosphoglycerate to ADP, thereby producing ATP [53]. The observed significant down-regulation of PTE expression may be related to the reduced energy demand of GP ♀ compared with GH.

4.4. DEPs Related to Lipid and Nucleotide Metabolism

Lipid and nucleotide metabolism is an important and complex biochemical process essential to life. The process involves digestion, absorption, synthesis, and decomposition, and it is promoted by a variety of related enzymes [54]. In the present study, DEPs related to purine metabolism (ko00230), fatty acid degradation (ko00071), and arachidonic acid metabolism (ko00590) were identified in the GP vs. GH comparison. Two proteins were significantly down-regulated in the GP vs. GH comparison: SDE and ADE. SDE exhibits high formaldehyde dehydrogenase activity in the presence of glutathione and catalyzes the oxidation of normal alcohols in a reaction independent of glutathione. Another study examined the changes in SDE expression in rabbits [55], but no studies have been conducted on aquatic animals, so the functional effects of SDE on both GP ♀ and GH generations deserve further investigation. ADE is an amino acid hydrolase that efficiently catalyzes the conversion of AMP to NH_3 and inosine. ADE is responsible for stabilizing adenylate-related energy changes. One study reported that copper ions reduce the activity of ADE in common carp *Cyprinus carpio* [56]. Another study found that the ADE activity of *Anguilla japonica* epithelial cells is higher [57]. Our research also suggests that more metabolic pathways can be activated compared with GP♀by increasing ADE expression in GH varieties.

5. Conclusions

GH generally displays intermediate growth rate characteristics between GP♀and GE♂. The survival rate of GH was significantly greater than that of its parents. Results of the TMT-based quantitative proteomic analysis suggest that DEPs significantly impact GH and its parents. In addition, the proteins expressed in GH showed fewer differences with GP♀but more differences with GE♂. KEGG pathway classification analysis revealed that most DEPs were the result of metabolic changes. The primary pathways identified included amino acid, carbohydrate, energy, lipid, and nucleotide metabolism. Regulation of the expression of proteins such as AHE, HRE, GCE, LDE, CKE, GFE, PKE, FAE, CAE, PHE, PTE, SDE, and AKE plays an important role in regulating the associated metabolic pathways. These proteins may be involved in the metabolic changes that underlie the growth superiority of GH over GP. The results of this study thus provide an important basis for selective breeding and improvement of GH.

Supplementary Materials: The following supporting information can be downloaded at: https://www.mdpi.com/article/10.3390/fishes9050158/s1, Table S1. Sequence information of primers used for qRT-PCR analysis.

Author Contributions: Conceptualization and methodology, Y.D. and Y.Z.; software and validation, Y.D.; formal analysis and resources, D.X. and Y.D.; data curation and writing—original draft preparation, Y.D.; writing—review and editing, J.Z.; visualization, Y.D. and D.Q.; project administration and funding acquisition, Y.D. and J.Z. All authors have read and agreed to the published version of the manuscript.

Funding: This work was supported by Research and Promotion of Key Technologies for hybrid Breeding and Culture of *Gymnocypris eckloni* and *Gymnocypris przewalskii* (22ZDYF0181); PhD Start-up Project of Xichang University (YBZ202240). The funders had no role in the study design, data collection and analysis, decision to publish, or preparation of the manuscript.

Institutional Review Board Statement: The study was conducted according to the guidelines of the Declaration of Helsinki and approved by the Animal Ethics Committee of Xichang University (Code: DKY20230314, Date: 10 August 2023).

Data Availability Statement: The data presented in this study are available on request from the corresponding author. The data are not publicly available due to privacy.

Conflicts of Interest: The authors declare no conflict of interest.

References

1. Wang, Y.S.; Gonzalez, R.J.; Patrick, M.L.; Grosell, M.; Wood, C.M. Unusual physiology of scale-less carp, *Gymnocypris przewalskii*, in Lake Qinghai: A high altitude alkaline saline lake. *Comp. Biochem. Physiol. Part A Mol. Integr. Physiol.* **2003**, *134*, 409–421. [CrossRef]
2. Yi, B.C.; Lan, W.U.; Lin, X.S.; Jun, P.Z.; Xiao, Y.E.; Xiao, Y.Z. Expression and purification of recombinant insulin-like growth factor-II of naked carp (*Gymnocypris przewalskii*) in lake Qinghai. *Acta Hydrobiol. Sin.* **2010**, *34*, 459–462. [CrossRef]
3. Cao, Y.B.; Chen, X.Q.; Wang, S.; Chen, X.C.; Wang, Y.X.; Chang, J.P. Growth hormone and insulin-like growth factor of naked carp (*Gymnocypris przewalskii*) in Lake Qinghai: Expression in different water environments. *Gen. Comp. Endocrinol.* **2009**, *161*, 400–406. [CrossRef]
4. Zhang, R.Y.; Ludwig, A.; Zhang, C.F.; Tong, C.; Li, G.G.; Tang, Y.T.; Peng, Z.G.; Zhao, K. Local adaptation of *Gymnocypris przewalskii* (*Cyprinidae*) on the Tibetan Plateau. *Sci. Rep.* **2015**, *5*, 9780. [CrossRef] [PubMed]
5. Zhao, K.; Li, J.B.; Yang, G.S.; Duan, Z.Y.; He, S.P.; Chen, Y.Y. Molecular phylogeny of endemic *Gymnocyprinus* in Qinghai lake and its adjacent water systems. *Chin. Sci. Bull.* **2005**, *50*, 1348–1355. (In Chinese) [CrossRef]
6. Qi, D.; Chao, Y.; Zhao, L. Complete mitochondrial genomes of two relatively closed species from *Gymnocypris* (*Cypriniformes: Cyprinidae*): Genome characterization and phylogenetic considerations. *Mitochondrial DNA* **2012**, *24*, 260–262. [CrossRef] [PubMed]
7. Wang, F.Y.; Wang, L.H.; Liu, D.; Gao, Q.; Nie, M.M.; Zhu, S.H.; Chao, Y.; Yang, C.J.; Zhang, C.F.; Yi, R.G.; et al. Chromosome-level assembly of *Gymnocypris eckloni* genome. *Sci. Data* **2022**, *9*, 464. [CrossRef]
8. O'Bryan, D.M.; Xie, Z.; Wang, Y. Phylogeography and conservation genetics of Lake Qinghai scaleless carp *Gymnocypris przewalskii*. *J. Fish Biol.* **2010**, *77*, 2072–2092. [CrossRef] [PubMed]
9. Yu, J.H.; Xia, D.Q.; Yang, H.; He, Y.H.; Wu, T.T. Morphology of the progenies of *Oreochromis aurea* (♀) × *Sinipperca chuatai* (♂). *J. Fish. China* **2003**, *27*, 431–435.
10. Zhu, S.R.; Ma, K.Y.; Xing, Z.J. The complete mitochondrial genome of and hybrid snakehead fish (*Channa maculata* ♀ × *Channa argus* ♂). *DNA Seq.* **2013**, *24*, 2. [CrossRef]
11. Li, Y.; Li, J.; Lu, J.; Li, Z.; Shi, S.; Liu, Z. Effects of live and artificial feeds on the growth, digestion, immunity and intestinal microflora of mandarin fish hybrid (*Siniperca chuatsi* ♀ × *Siniperca scherzeri* ♂). *Aquac. Res.* **2017**, *48*, 4479–4485. [CrossRef]
12. Won, E.T.; Douros, J.D.; Hurt, D.A.; Borski, R.J. Leptin stimulates hepatic growth hormone receptor and insulin-like growth factor gene expression in a teleost fish, the hybrid striped bass. *Gen. Comp. Endocrinol.* **2016**, *229*, 84–91. [CrossRef] [PubMed]
13. Diyaware, M.Y.; Modu, B.N.; Yakubu, U.P. Effect of different dietary protein levels on growth performance and feed utilization of hybrid catfish (*Heterobranchus bidorsalis* × *Clarias anguillaris*) fry in north-east Nigeria. *Afr. J. Biotechnol.* **2009**, *8*, 3954–3957. [CrossRef]
14. Wansuk, S.; Anne, R.; Uthairat, N.N.; Loren, M.M. Genetic impacts of hybrid catfish farming (*Clarias macrocephalus* × *C. gariepinus*) on native catfish populations in central Thailand. *Aquaculture* **2004**, *235*, 184. [CrossRef]
15. Prieto, M.; Silva, R.F.; Costa, L.S.; Pereira, R.T.; Rosa, P.V. Effect of fixed feeding time on growth, body composition, and hepatic histology of hybrid catfish (*Pseudoplatystoma reticulatum* × *Leiarius marmoratus*) fed with carbohydrates and lipids ratios. *Rev. Colomb. Cienc. Pecu.* **2015**, *28*, 83–92. [CrossRef]
16. Luo, S.W.; Luo, K.K.; Liu, S.J. A novel LEAP-2 in diploid hybrid fish (*Carassius auratus cuvieri* ♀ × *Carassius auratus* red var. ♂) confers protection against bacteria-stimulated inflammatory response. *Comp. Biochem. Physiol. Part C Toxicol. Pharmacol.* **2020**, *228*, 108665. [CrossRef] [PubMed]
17. Osuigwe, D.I.; Obiekezie, A.I.; Onuoha, G.C. Some haematological changes in hybrid catfish (*Heterobranchus longifilis* × *Clarias gariepinus*) fed different dietary levels of raw and boiled jackbean (*Canavalia ensiformis*) seed meal. *Afr. J. Biotechnol.* **2005**, *4*, 1017–1021. [CrossRef]
18. Wang, Y.D.; Yao, J.J.; Liao, A.M.; Tan, H.F.; Luo, Y.X.; Wu, P.; Wang, S.; Zhang, C.; Qin, Q.B.; Tao, M.; et al. The formation of hybrid fish derived from hybridization of *Megalobrama amblycephala* (♀) × *Siniperca chuatsi* (♂). *Aquaculture* **2022**, *548*, 737547. [CrossRef]
19. Welsh, E.A.; Stewart, P.A.; Chambers, M.C.; Zhang, G.; Fang, B.; Eschrich, S.A. Abstract 2708: Imputation-free analysis of high throughput TMT proteomics of 116 lung squamous samples. *Cancer Res.* **2018**, *78*, 2708. [CrossRef]
20. Nagami, K.; Mitsuzawa, S.; Mogi, A.; Ise, K.; Katsube, Y.; Esaki, H. Evaluation for a multicast extension of a label switching technology. *Electron. Commun. Jpn.* **2010**, *87*, 66–74. [CrossRef]
21. Hung, C.W.; Tholey, A. Tandem Mass Tag Protein Labeling for Top-Down Identification and Quantification. *Anal. Chem.* **2012**, *84*, 161–170. [CrossRef] [PubMed]

22. Men, L.; Li, Y.; Wang, X.; Li, R.; Gou, M. Protein biomarkers associated with frozen Japanese puffer fish (*Takifugu rubripes*) quality traits. *Food Chem.* **2020**, *327*, 127002. [CrossRef] [PubMed]
23. Konan, O.N.; D'Hont, A.; Baudoin, J.P.; Mergeai, G. Cytogenetics of a new trispecies hybrid in cotton: [(*Gossypium hirsutum* L. × *G. thurberi* Tod.)^2 × *G. longicalyx* Hutch. & Lee]. *Plant Breed.* **2010**, *126*, 176–181. [CrossRef]
24. Jiang, G.; Li, Q.; Xu, C.; Liu, S.; Yu, H. Reciprocal hybrids derived from *Crassostrea gigas* and *C. angulata* exhibit high heterosis in growth, survival and thermotolerance in northern China. *Aquaculture* **2021**, *73*, 7173. [CrossRef]
25. Potts, W.M.; Henriques, R.; Santos, C.V.; Munnik, K.; Ansorge, I.; Dufois, F. Ocean warming, a rapid distributional shift, and the hybridization of a coastal fish species. *Glob. Chang. Biol.* **2014**, *20*, 2765–2777. [CrossRef] [PubMed]
26. Li, Z.; Tian, Y.; Li, L.; Wu, Y.; Zhai, J. Characterization of the complete mitochondrial genome of the hybrid grouper *Epinephelus akaara* ♀ × *Epinephelus tukula* ♂, with its phylogenetic analysis. *Mitochondrial DNA Part B* **2019**, *4*, 3350–3351. [CrossRef] [PubMed]
27. Gaylord, T.G.; GatlinIii, D.M. Dietary lipid level but notl-carnitine affects growth performance of hybrid striped bass (*Morone chrysops* ♀ × *M. saxatilis* ♂). *Aquaculture* **2000**, *190*, 237–246. [CrossRef]
28. Dunham, R.A.; Argue, B.J. Seinability of Channel Catfish, Blue Catfish, and Their F_1, F_2, F_3, and Backcross hybrids in Earthen Ponds. *Progress. Fish Cult.* **1998**, *60*, 214–220. [CrossRef]
29. De-Assis, L.A.; Rezende, T.T.; Dias, M.A.D.; De Freitas, M.A.F.; Hilsdorf, R.T.S.; Wagner, A. The development of genetically improved red tilapia lines through the backcross breeding of two *Oreochromis niloticus* strains. *Aquaculture* **2017**, *472*, 17–22. [CrossRef]
30. He, S.; Liang, X.F.; Sun, J.; Li, L.; Yu, Y.; Huang, W.; Qu, C.M.; Cao, L.; Bai, X.L.; Tao, Y.X. Insights into food preference in hybrid F_1 of *Siniperca chuatsi* (♀) × *Siniperca scherzeri* (♂) mandarin fish through transcriptome analysis. *BMC Genom.* **2013**, *14*, 601. [CrossRef]
31. Hedgecock, D.; Lin, J.Z.; de-Cola, S.; Haudenschild, C.D.; Meyer, E.; Manahan, D.T.; Bowen, B. Transcriptomic analysis of growth heterosis in larval Pacific oysters (*Crassostrea gigas*). *Proc. Natl. Acad. Sci. USA* **2007**, *104*, 2313–2318. [CrossRef] [PubMed]
32. Zhao, Y.; Zhou, J.; Dong, Y.; Xu, D.; Qi, D. Transcriptome analysis reveals the molecular mechanisms underlying growth superiority in a novel *Gymnocypris* hybrid, *Gymnocypris przewalskii* ♀ × *G. eckloni* ♂. *Genes* **2024**, *15*, 182. [CrossRef]
33. Kaushik, S.J.; Seiliez, I. Protein and amino acid nutrition and metabolism in fish: Current knowledge and future needs. *Aquac. Res.* **2010**, *41*, 322–332. [CrossRef]
34. Tolin, S.; Arrigoni, G.; Trentin, A.R.; Veljovic-Jovanovic, S.; Pivato, M.; Zechman, B. Biochemical and quantitative proteomics investigations in Arabidopsis ggt1 mutant leaves reveal a role for the gamma-glutamyl cycle in plant's adaptation to environment. *Proteomics* **2013**, *13*, 2031–2045. [CrossRef] [PubMed]
35. Naderi, M.; Keyvanshokooh, S.; Ghaedi, A.; Salati, A.P. Effect of acute crowding stress on rainbow trout (*Oncorhynchus mykiss*): A proteomics study. *Aquaculture* **2018**, *495*, 106–114. [CrossRef]
36. Cramer, S.D.; Ferree, P.M.; Kai, L.; Milliner, D.S.; Holmes, R.P. The gene encoding hydroxypyruvate reductase (GRHPR) is mutated in patients with primary hyperoxaluria type II. *Hum. Mol. Genet.* **1999**, *8*, 2063–2069. [CrossRef]
37. Sloan, J.S.; Schwartz, B.W.; Becker, W.M. Promoter analysis of a light-regulated gene encoding hydroxypyruvate reductase, an enzyme of the photorespiratory glycolate pathway. *Plant J.* **2010**, *3*, 867–874. [CrossRef]
38. Gross, W. Occurrence of glycolate oxidase and hydroxypyruvate reductase in *Egregia menziesii* (Phaeophyta). *J. Phycol.* **2010**, *26*, 381–383. [CrossRef]
39. Solis, W.A.; Dalton, T.P.; Dieter, M.Z.; Freshwater, S.; Nebert, D.W. Glutamate-cysteine ligase modifier subunit: Mouse Gclm gene structure and regulation by agents that cause oxidative stress. *Biochem. Pharmacol.* **2002**, *63*, 1739–1754. [CrossRef] [PubMed]
40. Hicks, L.M.; Cahoon, R.E.; Bonner, E.R.; Rivard, R.S.; Sheffield, J.; Jez, J.M. Thiol-based regulation of redox-active glutamate-cysteine ligase from *Arabidopsis thaliana*. *Plant Cell* **2007**, *19*, 2653–2661. [CrossRef]
41. Zhou, J.M.; Li, N.; Wang, H.; Wang, C.; Mu, C. iTRAQ-based quantitative proteomic analysis reveals metabolic changes in overwintering *Scylla paramamosain* at two different salinities. *Aquac. Res.* **2021**, *52*, 3757–3770. [CrossRef]
42. Zhou, J.M.; Li, N.; Wang, H.; Wang, C.; Mu, C.; Shi, C. Effects of salinity on growth, nutrient composition, fatty acid composition and energy metabolism of *Scylla paramamosain* during indoor overwintering. *Aquac. Res.* **2020**, *51*, 1834–1843. [CrossRef]
43. Lee, H.K.; Maita, M.; Fukuda, Y.; Okamoto, N. Application of creatine kinase isoenzymes for detecting pathophysiological changes in yellowtail infected with *Lactococcus garvieae*. *Fish Pathol.* **2009**, *34*, 53–57. [CrossRef]
44. Lin, J.; Liao, Y.; Li, X.; Lu, K.; Song, K.; Wang, L. Effects of dietary creatine levels on the growth, muscle energy metabolism and meat quality of spotted seabass (*Lateolabrax maculatus*) fed low-fishmeal diets. *Aquaculture* **2023**, *565*, 739075. [CrossRef]
45. Zhou, H.; Sun, L.H.; Li, J.; Xu, C.Y.; He, J.H. The crystal structure of human GDP-L-fucose synthase. *Acta Biochim. Biophys. Sin.* **2013**, *45*, 720–725. [CrossRef] [PubMed]
46. Li, N.; Zhou, J.M.; Wang, H.; Mu, C.; Wang, C. Transcriptome analysis of genes and pathways associated with metabolism in *Scylla paramamosain* under different light intensities during indoor overwintering. *BMC Genom.* **2020**, *21*, 775. [CrossRef]
47. Zhou, J.M.; Li, N.; Wang, H.; Mu, C.; Wang, C. Transcriptome analysis reveals hepatopancreatic genes and pathways associated with metabolism responding to water salinities during the overwintering of mud crab *Scylla paramamosain*. *Aquac. Res.* **2021**, *52*, 3212–3225. [CrossRef]
48. Kuehn, A.; Hilger, C.; Lehners-Weber, C.; Codreanu-Morel, F.; Morisset, M.; Metz-Favre, C. Identification of enolases and aldolases as important fish allergens in cod, salmon and tuna: Component resolved diagnosis using parvalbumin and the new allergens. *Clin. Exp. Allergy* **2013**, *43*, 811–822. [CrossRef] [PubMed]

49. Nakamura, R.; Satoh, R.; Nakajima, Y.; Kawasaki, N.; Yamaguchi, T.; Sawada, J.I. Comparative study of GH-transgenic and non-transgenic amago salmon (*Oncorhynchus masou ishikawae*) allergenicity and proteomic analysis of amago salmon allergens. *Regul. Toxicol. Pharmacol.* **2009**, *55*, 300–308. [CrossRef]
50. Nemova, N.N.; Meshcheryakova, O.V.; Churova, M.V.; Murzina, S.A. Characteristics of the energy metabolism of the White Sea herring *Clupea pallasii marisalbi* Berg (*Clupeiformes, Clupeidae*) of Onega Bay, Dvina Bay, and Kandalaksha Bay of the White Sea. *Dokl. Biol. Sci.* **2016**, *469*, 173–177. [CrossRef]
51. Henry, R.P.; Gehnrich, S.; Weihrauch, D.; Towle, D.W. Salinity-mediated carbonic anhydrase induction in the gills of the euryhaline green crab, *Carcinus maenas*. *Comp. Biochem. Physiol. Part A Mol. Integr. Physiol.* **2003**, *136*, 243–258. [CrossRef] [PubMed]
52. Sun, B.; Wang, Z.; Zhu, F. Molecular cloning of kuruma shrimp *Marsupenaeus japonicus* phosphopyruvate hydratase and its role in infection by white spot syndrome virus and *Vibrio alginolyticus*. *Aquaculture* **2016**, *455*, 87–96. [CrossRef]
53. Cheung, C.W.; Mas, M.T. Substrate-induced conformational changes in yeast 3-phosphoglycerate kinase monitored by fluorescence of single tryptophan probes. *Protein Sci.* **2010**, *5*, 1144–1149. [CrossRef]
54. Dupuy, A.M.; Mas, E.; Ritchie, K.; Descomps, B.; Badiou, S.; Cristol, J.P. The Relationship between Apolipoprotein E4 and Lipid Metabolism Is Impaired in Alzheimer's Disease. *Gerontology* **2001**, *47*, 213–218. [CrossRef] [PubMed]
55. Keung, W.M.; Kunze, L.; Holmquist, B. Rabbit liver class III alcohol dehydrogenase: A cathodic Isoform with formaldehyde dehydrogenase activity. *Alcohol. Clin. Exp. Res.* **1995**, *19*, 860–866. [CrossRef]
56. Paecz, D.; Paecz, D.; Jaszczuk, E.; Jaszczuk, E.; Gabryelak, T.; Gabryelak, T. In vitrostudy of AMP-deaminase from fish (*Cyprinus carpio*) treated with hydrolyzable tannins. *Acta Biol. Hung.* **2006**, *57*, 49–56. [CrossRef]
57. Chan, D.K.O.; Wong, C.K.C. Functional partition of cells in the gill epithelium of the Japanese eel, *Anguilla japonica*, and the role of hormones. *Fish Physiol. Biochem.* **1997**, *17*, 405–413. [CrossRef]